

Energy-energy correlations in electron-positron annihilation

Lowell S. Brown and Stephen D. Ellis

Department of Physics, FM-15, University of Washington, Seattle, Washington 98195

(Received 26 May 1981)

The theoretical and experimental status of energy-energy correlations in high-energy electron-positron annihilation is reviewed. The importance of measuring structure with respect to external, laboratory directions is emphasized.

Energy-weighted cross sections involving the "antenna pattern"¹ and the energy-energy correlation^{2,3} have been proposed as sensitive and, in principle, unambiguous tests of quantum chromodynamics in high-energy electron-positron annihilation.⁴ Since the theory is asymptotically free, and since the energy weighting removes potential mass singularities, these cross sections can be computed using perturbation theory. This has been done in Refs. 1–3. These perturbative cross sections vanish slowly as the total electron-positron energy W increases; they vanish as $1/\ln W$ (relative to the total cross section). This slow energy behavior is to be contrasted with the energy dependence of the nonperturbative, quark-fragmentation corrections, which vanish at least as rapidly as $1/W$. Thus, at sufficiently high energies, the perturbative cross section stands out far above the nonperturbative fragmentation background, and a clear test of the fundamental theory of quantum chromodynamics becomes possible. Furthermore, for these energy-weighted cross sections, the nonperturbative background is itself easily estimated using standard phenomenological ideas.

The energy-energy correlation cross section provides a particularly good test of the theory because it has no zeroth-order contribution—the cross section arises (in leading order) from single-gluon emission, which vanishes as $1/\ln W$, and from fragmentation corrections to the zeroth-order process, which vanish as $1/W$. Recently, the PLUTO collaboration has presented data⁵ on the energy-energy cross section averaged over all orientations with respect to the beam direction but with the angle χ between the two correlated directions held fixed. It is the purpose of this paper to show that these data agree well with previous predictions³ and, encouraged by this agreement, to point out that a more precise comparison of theory and experiment can be performed. This can be accomplished by the measurement of the three independent structure functions which are contained in the energy-energy correlation cross section, for only one of these functions suffers from significant fragmentation corrections.

The energy-energy correlation cross section was

previously defined in terms of an experiment performed with a pair of calorimeters. It can, of course, also be determined in terms of measurements made on all the pairs of hadrons produced in each event. This latter method can be applied to existing data,⁵ and it helps clarify the meaning of the cross section. Consider first the average correlation cross section $d\Sigma/d\cos\chi$ obtained from the full energy-energy correlation by summing over all external angles but keeping the opening angle of the pair, χ , fixed. In terms of energy-weighted hadron pairs, it is defined by

$$\frac{1}{\sigma} \frac{d\Sigma}{d\cos\chi} \Delta\chi = \frac{2}{\sin\chi NW^2} \sum_{A=1}^N \sum_{\text{pairs in } \Delta\chi} E_{Aa} E_{Ab}. \quad (1)$$

The sums are to be performed as follows. The individual events are labeled by A , $A=1, 2, \dots, N$. In the A th event, all pairs of particles (a, b) are found which lie in the angular region χ to $\chi + \Delta\chi$, where χ is the angle between the directions of the members of the pair. The product $E_{Aa} E_{Ab}$ of the energies of the members of each pair is formed and summed over all distinct pairs ab . Finally, the sum over all events is taken. Note that each distinct pair of particles is counted only once while an individual particle may contribute in several pairs. The explicit factor 2 plus the inclusion of self-correlations ($\sum_a E_{Aa}^2$) at $\chi=0$ ensures the normalization³

$$\int d\cos\chi \frac{1}{\sigma} \frac{d\Sigma}{d\cos\chi} = 1. \quad (2)$$

In Eqs. (1) and (2) σ is the total annihilation cross section into hadrons with total energy W .

The first order of perturbation theory corresponds to the graphs shown in Fig. 1. Defining

$$\zeta = \frac{1}{2}(1 - \cos\chi), \quad (3)$$

the cross section can be written as

$$\frac{1}{\sigma} \frac{d\Sigma^{(1)}}{d\cos\chi} = \frac{\alpha_s(W)}{6\pi} \frac{3 - 2\zeta}{\zeta^5(1 - \zeta)} \times [3\zeta(2 - 3\zeta) + 2(3 - 6\zeta + 2\zeta^2) \ln(1 - \zeta)]. \quad (4)$$

Here $\alpha_s(W)$ is the usual running coupling

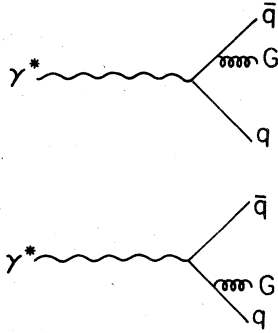


FIG. 1. Perturbative quantum-chromodynamic diagrams which yield Eqs. (4) and (5) for $\chi \neq 0, \pi$.

$$\alpha_s(W) = \frac{2\pi}{(11 - \frac{2}{3}N_f) \ln(W/\Lambda)} \quad (5)$$

with N_f the number of quark flavors and Λ the fundamental scale parameter. The perturbative cross section is singular for back-to-back and front-to-front correlations. Near the backward region we have

$$\frac{1}{\sigma} \frac{d\Sigma^{(1)}}{d \cos\chi} \xrightarrow{\xi \rightarrow 1} \frac{\alpha_s(W)}{3\pi} \left[\ln\left(\frac{1}{1-\xi}\right) - \frac{3}{2} \right] \frac{1}{1-\xi}. \quad (6)$$

This singularity arises from the "observation" of the quark and antiquark with the gluon becoming both soft and collinear. Near the forward region we have

$$\frac{1}{\sigma} \frac{d\Sigma^{(1)}}{d \cos\chi} \xrightarrow{\xi \rightarrow 0} \frac{\alpha_s(W)}{4\pi} \frac{1}{\xi}. \quad (7)$$

This weaker singularity arises from the "observation" of the quark (or antiquark) and a collinear gluon which is not soft. Although these singularities show that the perturbative development breaks down at large and small opening angles χ , it is valid in the intermediate angular region. In this intermediate region a reflection of the singularities is seen as a marked asymmetry about $\chi = \pi/2$.

The leading nonperturbative contribution can be derived³ by considering the hadronic fragmentation of the lowest-order process where only a quark and antiquark are produced. It is assumed that the fragmentation yields a distribution of hadrons characterized by a scaling behavior in momenta along the initial quark direction and a strongly damped (cutoff) behavior in momenta transverse to this direction. Simple considerations³ then yield a leading quark-fragmentation contribution to the energy-energy correlation given by

$$\frac{1}{\sigma} \frac{d\Sigma^{(qf)}}{d \cos\chi} = \frac{C \langle h_T \rangle}{W \sin^3\chi} = \frac{C \langle h_T \rangle}{8W} [\xi(1-\xi)]^{-3/2}. \quad (8)$$

The quantity $\langle h_T \rangle$ is the average transverse momenta produced in the fragmentation process. Thus $\langle h_T \rangle/W$ characterizes the opening angle of a

"hadron jet." The coefficient C is a measure of the "density" of hadrons, specifically the slope of the average number of hadrons produced in the annihilation vs $\ln W$:

$$C \equiv \frac{d}{d \ln W} \langle n \rangle_{\text{tot}}. \quad (9)$$

Note in particular that Eq. (8) is symmetric about $\chi = \pi/2$ as expected for a basically two-jet final state. Asymmetries in the hadronic final state due to the fragmentation process will arise from ordinary hadronic correlations (resonances, clusters, etc.) within a single "jet" and are expected³ to be much smaller, falling as W^{-2} for large W . Thus the effects of fragmentation are minimized by measuring the asymmetry defined by

$$A(\chi) \equiv \frac{1}{\sigma} \left[\frac{d\Sigma}{d \cos\chi}(\pi - \chi) - \frac{d\Sigma}{d \cos\chi}(\chi) \right]. \quad (10)$$

It is the cross section defined in Eq. (1) that was measured recently by the PLUTO collaboration.⁵ These data, for $W = 7.7, 22,$ and 30 GeV are plotted in Figs. 2a, 2b, and 2c. In each case the short-dashed curve is the evaluation of the perturbative cross section, Eq. (3), with $\Lambda = 0.3$ GeV and $N_f = 4$ at 7.7 GeV while $N_f = 5$ at the two higher energies. [This corresponds to $\alpha_s(W) = 0.18$ at $W = 30$ GeV.] The solid curve is the result of including both Eq. (3) and the nonperturbative correction of Eq. (8) with $\langle h_T \rangle = 0.3$ GeV/ c and $C = 2.5$, which are the values suggested in Ref. 3. No attempt has been made to fit these parameters to the data. Indeed, all these parameters were obtained from quite separate data. We conclude that a remarkably good description of the data has been afforded by this formulation. Note, however, that even at the highest energy, quark-fragmentation effects are still quite important, corresponding to approximately 40% of the signal. To focus the analysis on the perturbative QCD contribution, the PLUTO group has studied^{5(b)} the asymmetry defined in Eq. (10). While the analysis is limited by statistical accuracy, there is a clear indication that the perturbative result is in good agreement with the data at 30 GeV and that the corrections behave as W^{-2} as was predicted.³

This first success at isolating purely perturbative effects suggests that it will soon be possible to perform even more detailed experimental analysis to separate effects due to the nonperturbative fragmentation process, which must be treated phenomenologically, from the perturbative contributions, which rest on a solid theoretical foundation. To describe these more sensitive measurements, let us first recall how the full energy-energy correlation cross section is defined. We imagine having two small calorimeters as shown

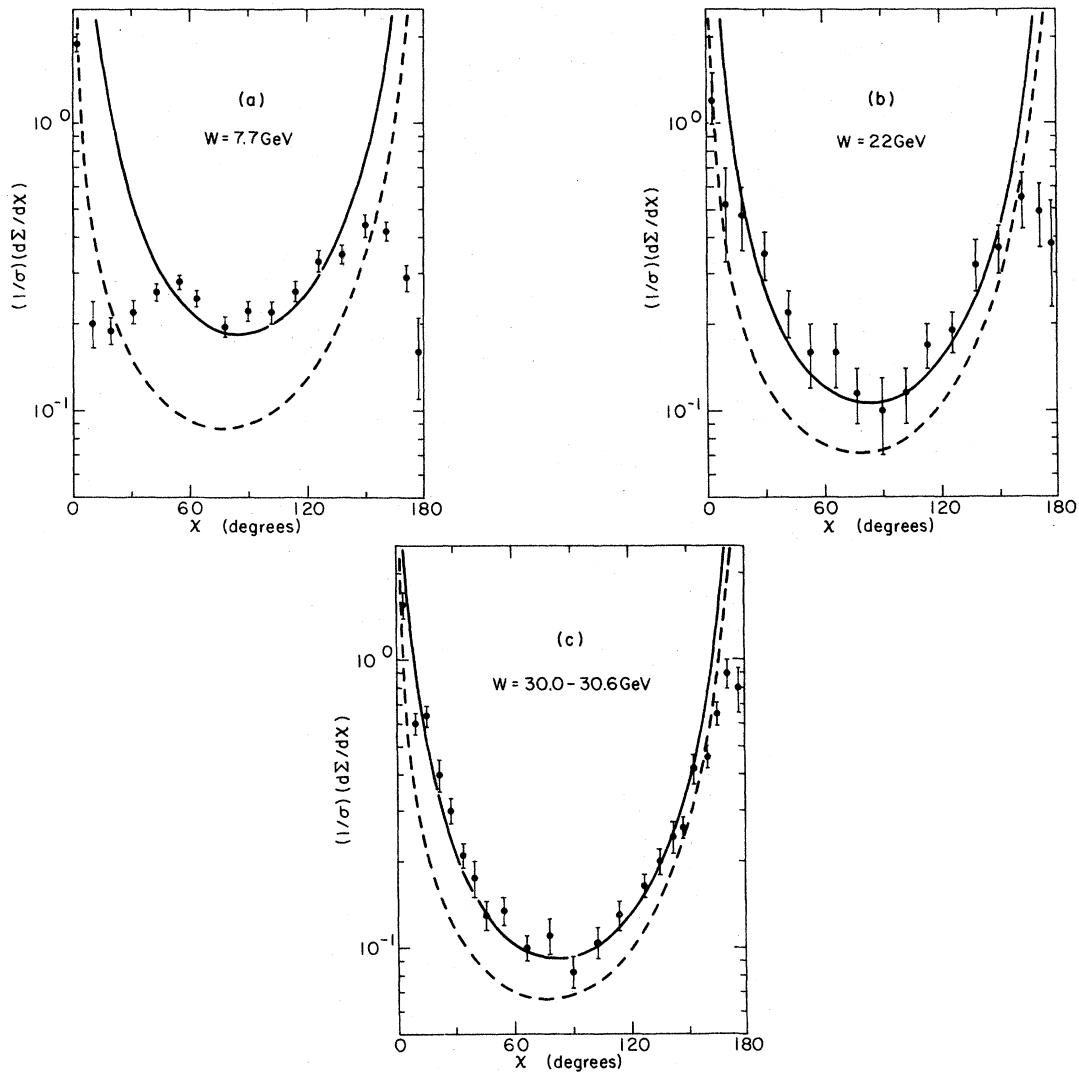


FIG. 2. Comparison of data from Ref. 5(a) with evaluation of Eqs. (4) and (8) for $(1/\sigma)d\Sigma/d\chi$ (not $d\Sigma/d\cos\chi$). The dashed curve is the purely perturbative result of Eq. (4). The full curve includes also the fragmentation correction, Eq. (10). The values of the parameters are $\Lambda = 0.3$ GeV, $C = 2.5$, $\langle h_T \rangle = 0.3$ GeV/c, and (a) $N_f = 4$ at 7.7 GeV; (b) $N_f = 5$ at 22 GeV; (c) $N_f = 5$ at 30 GeV. [Note that the data of Ref. 5(b) are normalized differently by a factor 2.]

in Fig. 3. Relative to the interaction region, one of the calorimeters subtends a small solid angle $d\Omega$ in the direction \hat{r} , the other a solid angle $d\Omega'$ in the direction \hat{r}' . A large number N of collisions are observed, with an individual collision labeled by A , $A = 1, 2, \dots, N$. The hadronic energies dE_A and dE'_A which enter into these calorimeters in the A th collision are measured. This procedure defines the full energy-energy correlation cross section $d^2\Sigma/d\Omega d\Omega'$ according to

$$\frac{1}{\sigma} \frac{d^2\Sigma}{d\Omega d\Omega'} = \frac{1}{N} \sum_{A=1}^N \left(\frac{dE_A}{W d\Omega} \right) \left(\frac{dE'_A}{W d\Omega'} \right). \quad (11)$$

The hadronic energy is produced by virtual photons giving a photon density matrix that contains

angular momentum two and zero. The coupling of this density matrix to the final hadronic system gives the energy-energy cross section an angular dependence on the detection directions \hat{r} and \hat{r}' relative to the external directions \hat{l} and \hat{b} of the beam and magnetic field. Since the angular momentum in the photon density matrix is limited, so is the complexity of this angular dependence. As is shown in Ref. 3, there are, in fact, only three independent terms in the energy-energy cross section which depend upon these external angles. For the general case in which the electron (positron) has a polarization P ($-P$) along the magnetic field direction, the energy-energy correlation cross section can be expressed as

$$\frac{1}{\sigma} \frac{d^2\Sigma}{d\Omega d\Omega'} = \frac{3}{8\pi} (\mathcal{Q}(\chi) \{P^2[2 - (\hat{r} \cdot \hat{b})^2 - (\hat{r}' \cdot \hat{b})^2] + \frac{1}{2}(1 - P^2)[2 + (\hat{r} \cdot \hat{l})^2 + (\hat{r}' \cdot \hat{l})^2]\} + \mathcal{R}(\chi) \{P^2[\cos\chi - (\hat{r} \cdot \hat{b})(\hat{r}' \cdot \hat{b})] + \frac{1}{2}(1 - P^2)[\cos\chi + (\hat{r} \cdot \hat{l})(\hat{r}' \cdot \hat{l})]\} + \mathcal{C}(\chi)). \quad (12)$$

The three structure functions \mathcal{Q} , \mathcal{R} , and \mathcal{C} depend only upon the angle χ between the detection directions \hat{r} and \hat{r}' with

$$\cos\chi = \hat{r} \cdot \hat{r}'. \quad (13)$$

Since a rather large number of external angles are involved in Eq. (12), we have chosen not to introduce new symbols for the external angular dependence but rather to write the cosines of these angles in terms of scalar products of the corresponding unit vectors. Thus, for example, $\hat{r} \cdot \hat{l} = \cos\theta$, where θ is the angle of the detector with respect to the beam direction as usually defined.

The more sensitive measurements alluded to above are those which separate the three intrinsic structure functions $\mathcal{Q}(\chi)$, $\mathcal{R}(\chi)$, and $\mathcal{C}(\chi)$ from the data. This is akin to the separation of the electric and magnetic form factors from the data on electron-proton scattering, and it can be performed by a least-squares or other statistical method. It should be emphasized that what is involved is the determination of three functions of a single variable, $\mathcal{Q}(\chi)$, $\mathcal{R}(\chi)$, and $\mathcal{C}(\chi)$, not a doubly differential cross section involving six angles. A simple calculation using Eq. (12) shows that the averaged correlation of Eq. (1) is given by

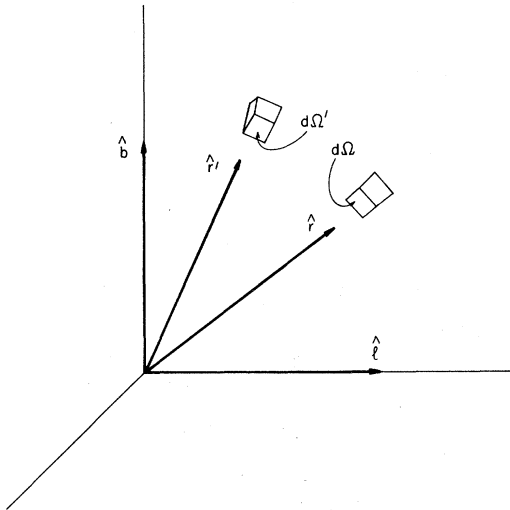


FIG. 3. Geometry for the full energy-energy correlation. Two small calorimeters subtending solid angles $d\Omega$ and $d\Omega'$ are positioned in the directions \hat{r} and \hat{r}' . The beam direction is denoted by \hat{l} and the direction of the magnetic field by \hat{b} .

$$\frac{1}{\sigma} \frac{d\Sigma}{d \cos\chi} = 2\pi [2\mathcal{Q}(\chi) + \cos\chi \mathcal{R}(\chi) + \frac{3}{2}\mathcal{C}(\chi)]. \quad (14)$$

The particular choice of the definition of the three structure functions presented in Eq. (12) leads to considerable theoretical simplicity and to useful distinctions between the properties of $\mathcal{Q}(\chi)$, $\mathcal{R}(\chi)$, and $\mathcal{C}(\chi)$.

The dependence on external angles exhibited by the first term in Eq. (12) [$\mathcal{Q}(\chi)$] arises naturally because it is the behavior exhibited by the zeroth-order cross section $d\sigma^{(0)}/d\Omega$ describing the production of a quark or antiquark in the direction \hat{r} . The coefficient of $\mathcal{Q}(\chi)$ is simply $(1/\sigma)[d\sigma^{(0)}/d\Omega + d\sigma^{(0)}/d\Omega']$. In first order in α_s , the squared matrix element for producing a quark in the direction \hat{r} and an antiquark in the direction \hat{r}' (or vice versa) is proportional to this angular factor. More important to the choice of \mathcal{Q} , however, is the fact that at high energies the largest nonperturbative correction from quark fragmentation, which is of order $1/W$, corresponds to a situation where the quark is emitted (in zeroth order) in the direction \hat{r} and a fragment of that quark ($\chi < \pi/2$), or of the opposite moving antiquark ($\chi > \pi/2$), appears in the direction \hat{r}' or to similar configurations where the roles of \hat{r} and \hat{r}' or quark-antiquark are reversed. Such contributions clearly depend on the external angles in the form $[d\sigma^{(0)}/d\Omega + d\sigma^{(0)}/d\Omega']$ and hence are part of $\mathcal{Q}(\chi)$. To leading order $[O(1/W)]$, only the $\mathcal{Q}(\chi)$ coefficient is corrected by quark fragmentation, with

$$\mathcal{Q}(\chi)^{(qf)} = \frac{C\langle h_T \rangle}{4\pi W \sin^3\chi}. \quad (15)$$

The first-order perturbative contribution corresponding to the production of a quark in the direction \hat{r} and a gluon in the direction \hat{r}' , with the antiquark recoiling in a third direction specified by momentum conservation, plus the analogous cases with quark, antiquark and/or \hat{r} , \hat{r}' interchanged is not simply proportional to $[d\sigma^{(0)}/d\Omega + d\sigma^{(0)}/d\Omega']$. It also exhibits a contribution involving the external angular behavior $P^2[\cos\chi - (\hat{r} \cdot \hat{b})(\hat{r}' \cdot \hat{b})] + \frac{1}{2}(1 - P^2)[\cos\chi + (\hat{r} \cdot \hat{l})(\hat{r}' \cdot \hat{l})]$. This additional structure is produced, for example, when \hat{r} is replaced by $-(\hat{r} + \hat{r}')$ in the angular behavior of $d\sigma^{(0)}/d\Omega$ written as $P^2[\hat{r} \cdot \hat{r} - (\hat{r} \cdot \hat{b})^2] + \frac{1}{2}(1 - P^2)[\hat{r} \cdot \hat{r} + (\hat{r} \cdot \hat{l})^2]$. This new direction arises because the direction of the recoiling antiquark (or quark) can always be expressed as having a component in the direction \hat{r} and a component in the direction $-(\hat{r} + \hat{r}')$. We

have chosen $\mathcal{G}(\chi)$ as the coefficient of this angular form. This choice ensures that the third independent term $[\mathcal{C}(\chi)]$, which involves only zero angular momentum in the photon density matrix, has its first contribution only in higher order.

Thus, with the specific choice of structure functions displayed in Eq. (12), we have a hierarchy of sizes characteristic of perturbative quantum chromodynamics and the usual picture of quark fragmentation: $\mathcal{G}(\chi)$ receives contributions starting at order α_s and $1/W$, $\mathcal{B}(\chi)$ receives contributions at order α_s , with no leading fragmentation correction of order $1/W$, and $\mathcal{C}(\chi)$ receives its first perturbative contribution⁶ at order α_s^2 and has no leading fragmentation correction of order $1/W$. This structure can be contrasted with, for example, a theory with scalar quarks which would instead exhibit leading contributions with external angular dependence involving the factors $[(\hat{\gamma} \cdot \hat{b})^2 + (\hat{\gamma}' \cdot \hat{b})^2]$ and $[(\hat{\gamma} \cdot \hat{b})(\hat{\gamma}' \cdot \hat{b})]$ for the simple case $P^2=1$. The specific behavior of the structure functions $\mathcal{G}(\chi)$, $\mathcal{B}(\chi)$, and $\mathcal{C}(\chi)$ in the single internal angular variable χ is, of course, also characteristic of the underlying physics.⁷

For the sake of completeness, let us record the specific forms of the structure functions derived³ in first-order perturbation theory:

$$\mathcal{G}^{(1)}(\chi) = \frac{\alpha_s(W)}{12\pi^2} \frac{1}{1-\xi} \left[\frac{(3-4\xi)}{\xi^5} \ln(1-\xi) + \frac{3}{\xi^4} - \frac{5}{2\xi^3} - \frac{1}{\xi^2} \right], \quad (16a)$$

$$\mathcal{B}^{(1)}(\chi) = \frac{\alpha_s(W)}{12\pi^2} \frac{1}{1-\xi} \left[\frac{4(1-\xi)(3-\xi)}{\xi^5} \ln(1-\xi) + \frac{12}{\xi^4} - \frac{10}{\xi^3} \right], \quad (16b)$$

and

$$\mathcal{C}^{(1)}(\chi) = 0. \quad (16c)$$

Note that the most singular behavior as $\xi \rightarrow 1$ arises solely from $\mathcal{G}^{(1)}(\chi)$ as it should since this term contains the total contribution from "observing" the quark and antiquark.

In summary, we are very much encouraged by the recent data on the hadronic energy correlation produced in high-energy e^+e^- annihilation. They agree well with the predictions of quantum chromodynamics. This test of the fundamental theory of strong interactions would be sharpened and strengthened with the experimental separation of

the individual structure functions $\mathcal{G}(\chi)$, $\mathcal{B}(\chi)$, and $\mathcal{C}(\chi)$.

Note added in proof. As observed in the text, the perturbative expansion in powers of $\alpha_s(W)$, for which Eq. (4) is the first term, breaks down in any fixed order as $\chi \rightarrow 0^\circ$ and as $\chi \rightarrow 180^\circ$. In the text we did not explicitly describe the extent of the angular regions where the first-order calculation ceases to be valid. We rectify that omission here. Although an analysis to all orders^{8,9} of perturbation theory is necessary to describe these singular regions in detail, a simple measure of the onset of the breakdown of the first-order result is provided by the most singular piece of the order- $\alpha_s(W)^2$ contribution. In the more singular region, $\chi \rightarrow 180^\circ$ or $\xi \rightarrow 1$, this piece is approximately⁸ $(\alpha_s/\pi) \times \ln^2(1-\xi)$ times the order- α_s limit displayed in Eq. (6). To obtain a specific (if somewhat arbitrary) numerical estimate of the range of validity of the first-order result at $W=30$ GeV, we note that for $\chi \gtrsim 145^\circ$ this correction factor is $\gtrsim 30\%$. In the less singular region, $\chi \rightarrow 0$ or $\xi \rightarrow 0$, the corresponding factor is approximately⁹ $(\alpha_s/\pi) \ln(1/\xi)$ which exceeds 30% only for the much smaller angular region $\chi \lesssim 10^\circ$. Note that the asymmetry about 90° of the range of validity of the first-order perturbation theory again illustrates the intrinsic asymmetry of the QCD process. Of course, the second-order contribution⁶ may be significant even in the restricted angular interval $10^\circ \lesssim \chi \lesssim 145^\circ$ at present energies, and this contribution must be included to obtain a definitive measurement of the QCD scale Λ . The nonperturbative, fragmentation correction given in Eq. (8) of the text is the leading term in a $1/W$ expansion which breaks down at small and large angles where $\langle h_T \rangle / (W \sin \chi)$ becomes of order unity. At $W=30$ GeV, this breakdown occurs only for χ within about 1° of $\chi=0$ or $\chi=180^\circ$, a much smaller angle than the corresponding perturbative cutoffs discussed above. The higher-order ($1/W^2$) fragmentation corrections, which may be rather asymmetrical about 90° , in contrast to the symmetrical ($1/W$) fragmentation correction, are expected to be quite small outside of these 1° regions for $W \gtrsim 30$ GeV.

ACKNOWLEDGMENTS

We are grateful for conversations with T. H. Burnett and H. Meyer. This work was supported in part by the U. S. Department of Energy under Contract No. DE-AC06-76ERO1388.

¹C. L. Basham, L. S. Brown, S. D. Ellis, and S. T. Love, Phys. Rev. D 17, 2298 (1978).

²C. L. Basham, L. S. Brown, S. D. Ellis, and S. T. Love, Phys. Rev. Lett. 41, 1585 (1978).

- ³C. L. Basham, L. S. Brown, S. D. Ellis, and S. T. Love, Phys. Rev. D 19, 2018 (1979).
- ⁴This work is reviewed by L. S. Brown, in *High-Energy Physics in the Einstein Centennial Year, 1979*, proceedings of Orbis Scientiae, Coral Gables, edited by A. Perlmutter, F. Krausz, and L. F. Scott (Plenum, New York, 1979).
- ⁵(a) V. Hepp, in *High Energy Physics—1980*, proceedings of the XXth International Conference, Madison, Wisconsin, edited by L. Durand and L. G. Pondrom (AIP, New York, 1981), p. 622; (b) Ch. Berger *et al.*, Phys. Lett. 99B, 292 (1981).
- ⁶S. D. Ellis and W. J. Stirling (in preparation).
- ⁷The structure functions for the emission of scalar gluons have been computed by C. L. Basham and S. T. Love, Phys. Rev. D 20, 340 (1979).
- ⁸The theoretical study of the $\chi \rightarrow 180^\circ$ limit is presently a very active field. See, e.g., C. L. Basham, L. S. Brown, S. D. Ellis, and S. T. Love, Phys. Lett. 85B, 297 (1979); S. D. Ellis, N. Fleishon, and W. J. Stirling, Phys. Rev. D 24, 1386 (1981); J. Collins and D. Soper, Report No. OTIS-155, 1981 (unpublished).
- ⁹See, e.g., K. Konishi, A. Ukawa, and G. Veneziano, Phys. Lett. 80B, 259 (1979); and, more in the present context, S. D. Ellis, in *Quantum Flavor Dynamics, Quantum Chromodynamics and Unified Theories*, NATO Advanced Study Institute, Boulder, Colorado, 1979, edited by K. T. Mahanthappa and J. Randa (Plenum, New York, 1980), p. 214.